

## Evolution of the Dendritic Instability in Solidifying Succinonitrile

Henry Chou and Herman Z. Cummins

Department of Physics, City College of the City University of New York, New York, New York 10031

(Received 27 October 1987)

The evolution of morphological instability in solidifying succinonitrile has been investigated with high-resolution videomicroscopy. Quantitative analysis of the early development of the instability has demonstrated the critical role of noise, and indicates significant disagreement with predictions of the Mullins-Sekerka theory. The ratio of the tip radius  $\rho^*$  of the steady-state dendrites to the length scale  $\lambda_{\max}$  of the initial instability was found to be approximately 0.5, in reasonable agreement with a recent theoretical prediction of Barbieri, Hong, and Langer.

PACS numbers: 68.70.+w, 61.50.Cj, 81.30.Fb

Morphological instabilities leading to pattern selection have recently received increasing attention, primarily stimulated by major theoretical advances.<sup>1,2</sup> The instability occurring at the interface of a crystal growing into its undercooled melt, leading to dendrites resembling the familiar snowflake structure, is of particular interest because of its significance in metallurgy and crystal growth.

In 1963, Mullins and Sekerka<sup>3</sup> carried out a linear stability analysis for this problem. The three equations governing solidification, (1) thermal diffusion, (2) energy conservation at the interface, and (3) the Gibbs-Thomson equation for the local melting temperature, were linearized and solved for an initially steady-state planar interface  $\xi_0 = v_0 t$  advancing at constant velocity  $v_0$  with a superimposed sinusoidal perturbation:  $\xi(\mathbf{r}) = \xi_0 + \xi_k e^{i\mathbf{k}\cdot\mathbf{r}} e^{\omega t}$ . The resulting linearized solution for the growth rate  $\omega(k)$  defines a stability curve:

$$\omega(k) \approx v_0 k (1 - d_0 l k^2), \quad (1)$$

where  $l = 2D/v_0$  is the thermal diffusion length and  $d_0 = \gamma T_M C_p / L^2$  is the capillary length. The thermodynamic parameters in  $l$  and  $d_0$  and their values for succinonitrile are<sup>4</sup>  $D$ =thermal diffusion constant =  $1.16 \times 10^{-3} \text{ cm}^2/\text{s}$ ;  $\gamma$ =crystal-melt surface tension =  $8.95 \text{ dyn/cm}$ ;  $T_M$ =bulk melting temperature =  $331.2 \text{ K}$ ;  $C_p$ =heat capacity =  $2.0 \times 10^7 \text{ erg/K cm}^3$ ;  $L$ =latent heat =  $4.63 \times 10^8 \text{ erg/cm}^3$ .

In obtaining the approximate result of Eq. (1), one assumes that  $D$  and  $C_p$  are the same for the solid and the melt (symmetric model),  $kl \gg 1$  and  $k\xi_k \ll 1$ . With the values given above and with  $v_0 = 4.5 \text{ }\mu\text{m/s}$ , we find  $l = 4.56 \text{ cm}$  and  $d_0 = 27.7 \times 10^{-8} \text{ cm}$ . The stability curve [Eq. (1)] with those values is shown in Fig. 1(a). The planar solidification front is always unstable ( $\omega_k > 0$ ) against small fluctuations for wave vectors  $0 < k < k_c = (d_0 l)^{-1/2}$ , with the maximum instability at  $k_{\max} = k_c / \sqrt{3} = (3d_0 l)^{-1/2}$  which establishes the length scale  $\lambda_{\max} = 2\pi/k_{\max}$  of the initial pattern. For succinonitrile,  $k_{\max} = 515 \text{ cm}^{-1} = 0.0515 \text{ }\mu\text{m}^{-1}$  as shown as Fig. 1(a), so that  $\lambda_{\max} = 112 \text{ }\mu\text{m}$ .

As the amplitude of the interfacial pattern evolves into the nonlinear regime where the Mullins-Sekerka analysis is no longer valid, a coarsening phenomenon occurs during which some protrusions advance as others are squeezed out. Eventually a steady-state pattern develops in which parallel dendrites with parabolic tips of radius  $\rho^*$ , separated by a spacing of  $\lambda_1^*$ , each emitting roughly periodic secondary dendrites, advance into the under-

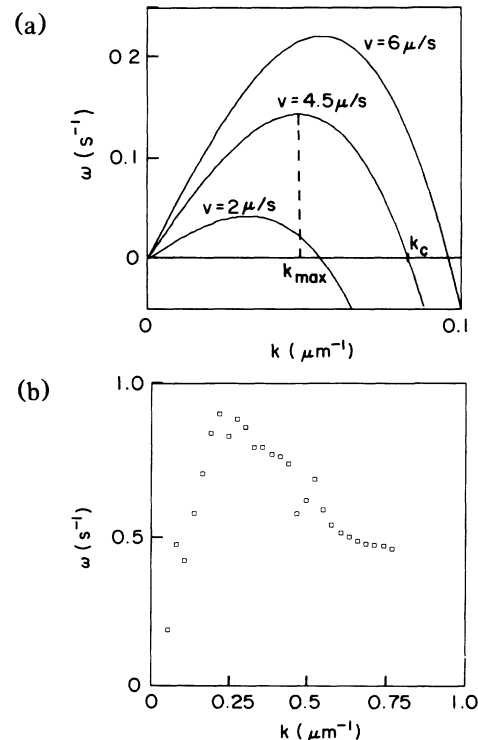


FIG. 1. (a) Mullins-Sekerka stability curve  $\omega$  vs  $k$  from Eq. (1) for succinonitrile with  $v_0 = 2, 4.5,$  and  $6 \text{ }\mu\text{m/s}$  and the thermodynamic parameters listed in the text. (b) Experimental growth rate curve for succinonitrile deduced from ensemble-averaged Fourier transforms of twelve interface profiles spanning 2.4 s of growth.

cooled melt at a uniform velocity  $v^*$ . The mechanism leading to the selection of unique values of  $\rho^*$ ,  $\lambda_1^*$ , and  $v^*$  for a given undercooling  $\Delta T$  has been the major focus of most recent research in this field.<sup>1,5-9</sup>

Recently, Barbieri, Hong, and Langer<sup>10</sup> gave an analytic solution of the problem of velocity selection in a fully *nonlocal* model of dendritic growth. They found that in two dimensions the selected tip radius  $\rho^*$  is given by

$$\rho^* \approx (d_0 l^* / \sigma_0)^{1/2} \alpha^{-7/8}, \quad (2)$$

where  $\sigma_0 \approx 1$ ,  $l^* = 2D/v^*$ , and  $\alpha$  is the anisotropy in the surface tension  $\gamma(\theta)$  which, for cubic crystals, is given by  $\gamma(\theta) = \bar{\gamma}[1 - \alpha \cos(4\theta)]$ . Combining Eq. (2) with the Mullins-Sekerka expression for the initial length scale  $\lambda_{\max}$  (and setting  $\sigma_0 = 1$ ), we have

$$\frac{\rho}{\lambda_{\max}} = \frac{1}{2\pi} \left( \frac{v_0}{3v^*} \right)^{1/2} \alpha^{-7/8}. \quad (3)$$

Huang and Glicksman<sup>11</sup> observed the equilibrium shape of liquid droplets in a crystal of pure succinonitrile and found 1.4% variation in radius attributed to anisotropy. If  $r(\theta) = r_0[1 + \beta \cos(4\theta)]$ , this measurement implies that  $\beta \approx 0.007$ . As noted by Kessler, Koplik, and Levine,<sup>2</sup> the surface-tension anisotropy  $\alpha$  is larger than the energy anisotropy (which determines the shape) by a factor of  $n^2 - 1$  where  $n$  is the order of the crystalline rotational symmetry axis. For cubic succinonitrile,  $n = 4$ ,  $n^2 - 1 = 15$ , and  $\alpha \approx 0.105$ .

Several experimental studies have been conducted to test various predictions of these and earlier theories. The seminal studies of succinonitrile by Glicksman, Schaefer, and Ayers<sup>4</sup> determined the tip radius and growth velocity as functions of undercooling. Their results were found to agree remarkably well with the marginal-stability hypothesis.<sup>1</sup> A number of other experiments have been carried out to study  $\rho^*$  and  $v^*$  as functions of undercooling or impurity concentration.<sup>12-18</sup>

We have undertaken a detailed quantitative study of the morphological instability in solidifying succinonitrile in order to test both the Mullins-Sekerka theory and some recent predictions for the characteristics of the steady-state dendritic pattern and their relation to crystalline anisotropy. Our apparatus, based on the temperature gradient microscope of Hunt and co-workers,<sup>19,20</sup> employs a Nikon diaphot inverted microscope with Nomarski optics equipped with a video camera (MTI-Dage series 68 Nuvison) which provides a  $512 \times 480$ -pixel image at 30 frames/s. One pixel corresponds to  $0.96 \mu\text{m}$  in the sample. The video signal is either recorded on a video cassette recorder or directed to a Plessey model LSI-11/73 computer equipped with a real-time digital image-processing system (Imaging Technology series 512) consisting of a frame buffer and a feature-extraction module.

Our samples are prepared from 99% pure succinonitrile  $[(\text{CH}_2\text{CN})_2]$  (Fluka Chemical Corporation), load-

ed by capillary action into cells made from two microscope cover slides epoxied together. A film of evaporated aluminum along three edges of one slide acts as a spacer producing a uniform cell thickness, typically  $\approx 5 \mu\text{m}$ . The cell is placed across two thermostatted blocks separated by 0.64 cm, one above ( $95^\circ\text{C}$ ) and one below ( $45^\circ\text{C}$ ) the melting temperature  $T_M = 58^\circ\text{C}$ , producing an (initially) planar interface oriented to appear as a vertical bright line on a dark background on the video monitor. To initiate the experiment, the hot block is chilled by a thermoelectric cooler at  $0.4^\circ\text{C/s}$ . Ideally, the crystal should grow into a uniformly undercooled melt which is only approximated in our apparatus. After an initial delay, the interface begins to move horizontally, and soon develops small, approximately sinusoidal, fluctuations that grow and proceed through coarsening to a final steady-state dendritic pattern.

The feature-extraction module is programmed to extract the coordinates and intensities of all pixels whose intensity is above a specified threshold and pass them to the computer memory. With this procedure we are able to perform real-time feature analysis at 5 frames/s. The location of the interface is determined for each scan line by an interpolation procedure similar to that of Dougherty, Kaplan, and Gollub.<sup>14</sup> A parabola is fitted to the intensity values of the recorded points on each scan line and the position of the fitted maximum is *defined* as the position of the interface. With this procedure, the interface position can be determined to within  $0.2 \mu\text{m}$ , as shown in Fig. 2 for times of 2, 3, and 4 s after the onset of the motion. The interface coordinates are next smoothed by fitting with a least-squares cubic *B*-spline routine over ten points at a time.<sup>21</sup> The resulting smooth curves are shown by the solid lines in Fig. 2. After this procedure, the shortest meaningful wavelength of fluctuation that can be analyzed is  $\approx 6 \mu\text{m}$ , corresponding to a maximum significant  $k$  value of  $1 \mu\text{m}^{-1}$ .

The spline-fitted smooth curves are then (spatial) Fourier transformed with a fast-Fourier-transform algorithm.<sup>21</sup> Fourier spectra corresponding to the interface data of Fig. 2 are shown in Fig. 3. The important Fourier components lie within a limited range of  $k$  values as predicted, but the spectra are surprisingly noisy. The variation in Fourier amplitudes among components with nearly equal  $k$  values, which are theoretically equally unstable and should grow at the same rate, shows that the initial growth of individual Fourier components must be stochastic, driven by noise in the system which determines which components begin to grow first. A similar conclusion was reached by Dougherty, Kaplan, and Gollub for the launching of side branches in fully developed dendrites,<sup>14</sup> and by Meyer, Ahlers, and Cannell for the Rayleigh-Bénard instability.<sup>22</sup>

In order to compare our data with the predictions of the linear-stability analysis of Mullins and Sekerka, we need to determine the growth rate of each Fourier component, which should not reflect the irregularity of the

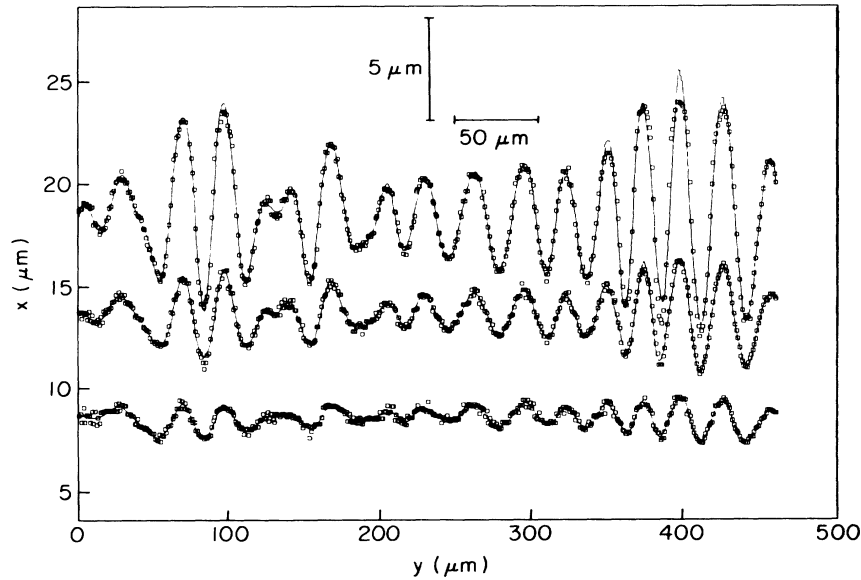


FIG. 2. Experimental interface profiles  $x(y)$  obtained by interpolation 2, 3, and 4 s after onset of interface motion ( $t=0$ ,  $x=0$ ). The solid lines through the data points are ten-point least-squares cubic  $B$ -spline fits. Note the scale difference between the  $x$  and  $y$  axes indicated by the inset horizontal and vertical bars.

Fourier amplitudes. To accomplish this, we first averaged Fourier spectra of ten 200- $\mu\text{m}$  segments of the recorded interface, each successively displaced by 10  $\mu\text{m}$ , in order to smooth partially the extreme noise due to the stochastic initial conditions. This averaging procedure was applied to twelve video frames spanning 2.4 s of real time, which were then Fourier transformed. The growth rate was deduced from the resulting averaged Fourier amplitudes by the fitting of the amplitude  $\xi_k(t)$  by

$\xi_k(t) = \xi_k(0)\exp(\omega_k t)$ . The resulting experimental growth-rate curve ( $\omega_k$  vs  $k$ ) is shown by the points in Fig. 1(b). For the particular run analyzed here, the average interface velocity was nearly constant at  $v_0 \approx 4.5 \mu\text{m/s}$  throughout the 2.4 s of data collection.

The experimental growth-rate curve is qualitatively similar to the theoretical Mullins-Sekerka stability curve, but its peak is at  $k_{\text{max}} \approx 0.2 \mu\text{m}^{-1}$  corresponding to an experimental  $\lambda_{\text{max}} \approx 30 \mu\text{m}$  rather than the predicted 112  $\mu\text{m}$ .

There are several possible explanations for this discrepancy. First, diffusion of impurities can modify the morphological instability by changing  $d_0$  and  $l$ .<sup>18</sup> However, recent experiments with cells loaded in vacuum with multiply distilled material gave essentially identical results. Second, the sample-cell thickness could play a role here as a result of wetting effects as was demonstrated recently by Fattinger, Honegger, and Lakosz.<sup>23</sup> To test this possibility we prepared cells of thickness 25 and 50  $\mu\text{m}$  and repeated the experiment. The 25- $\mu\text{m}$  cell gave essentially the same results as the 5- $\mu\text{m}$  cell. In the 50- $\mu\text{m}$  cell the final dendrites appeared to be three dimensional, but there was no significant change in the length scale of the initial instability. Finally, we note that the analysis leading to Eq. (1) assumes that the crystal grows into a uniformly undercooled melt at steady state, whereas in our apparatus the undercooling is both position and time dependent. This distinction is probably crucial since a positive temperature gradient acts to stabilize the interface. Quantitative theoretical analysis of the nonuniformly undercooled case is currently in progress and will be reported

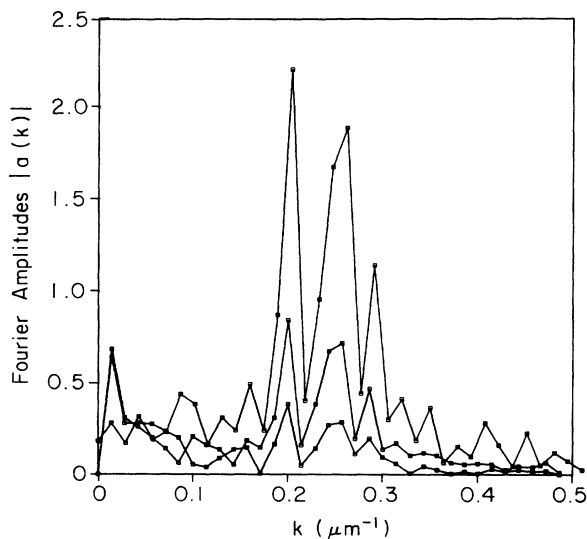


FIG. 3. Modulus of (fast-Fourier-transform) Fourier coefficients of the data of Fig. 2.

in a subsequent communication.

We have also followed the evolution of the interfacial pattern through the coarsening stage to the final steady-state dendritic structure. After about 20 s, side branching begins. After approximately 30 s, the steady state is achieved with an array of parallel dendrites advancing with growth velocity of  $v^* \approx 45 \mu\text{m/s}$ . Equation (5) (with  $v_0/v^* = 0.1$  and  $\alpha = 0.105$ ) thus predicts that  $\rho^*/\lambda_{\text{max}} \approx 0.21$ . The observed final tip radius was  $\rho^* \approx 16 \mu\text{m}$ , so that the experimental value of  $\rho^*/\lambda_{\text{max}} \approx 0.5$ .<sup>24</sup> The primary dendrite spacing at steady state was  $\lambda_1^* \approx 350 \mu\text{m}$ , so that the coarsening (taken as  $\lambda_1^*/\lambda_{\text{max}}) \approx 10$ .

Given that the anisotropy  $\alpha$  is only known approximately, our value of  $\rho^*/\lambda_{\text{max}} = 0.5$  is in reasonably agreement with the prediction of Barbieri, Hong, and Langer.<sup>10</sup> Further tests of this prediction with other materials with different anisotropies would be useful as would a further analysis of the Mullins-Sekerka region with a uniformly undercooled melt.

We wish to acknowledge helpful discussions with K. A. Jackson, H. Levine, A. Libchaber, J. P. Gollub, M. Lax, H. Falk, B. Shraiman, W. van Saarloos, M. E. Glicksman, J. D. Weeks, O. Martin, X. W. Qian, and M. Muschol. This research was supported by the U.S. Department of Energy under Grant No. DE-FG02-84ER45132.

<sup>1</sup>J. S. Langer, *Rev. Mod. Phys.* **52**, 1 (1980).

<sup>2</sup>D. A. Kessler, J. Koplik, and H. Levine, *Adv. Phys.* (to be published).

<sup>3</sup>W. W. Mullins and R. F. Sekerka, *J. Appl. Phys.* **34**, 323 (1963), and **35**, 444 (1964).

<sup>4</sup>M. E. Glicksman, R. J. Schaefer, and J. D. Ayers, *Metall. Trans.* **7A**, 1747 (1976).

<sup>5</sup>J. S. Langer and H. Müller-Krumbhaar, *J. Crystal. Growth* **42**, 11 (1977), and *Acta Metall.* **26**, 1681, 1689, 1697 (1978).

<sup>6</sup>D. Kessler and H. Levine, *Phys. Rev. B* **33**, 7687 (1986); D. Kessler, J. Koplik, and H. Levine, *Phys. Rev. A* **33**, 3352 (1986).

<sup>7</sup>E. Ben-Jacob, N. Goldenfeld, J. S. Langer, and G. Schön, *Phys. Rev. Lett.* **51**, 1930 (1983), and *Phys. Rev. A* **29**, 330 (1984).

<sup>8</sup>J. S. Langer and D. C. Hong, *Phys. Rev. A* **34**, 1462 (1986).

<sup>9</sup>J. D. Weeks and W. van Saarloos, *Phys. Rev. A* **35**, 3001 (1987).

<sup>10</sup>A. Barbieri, D. C. Hong, and J. S. Langer, *Phys. Rev. A* **35**, 1802 (1987).

<sup>11</sup>S. C. Huang and M. W. Glicksman, *Acta Metall.* **29**, 701, 717 (1981); M. E. Glicksman, private communication.

<sup>12</sup>H. Honjo and Y. Sawada, *J. Cryst. Growth* **58**, 297 (1982).

<sup>13</sup>H. Honjo, S. Ohta, and Y. Sawada, *Phys. Rev. Lett.* **55**, 841 (1985).

<sup>14</sup>A. Dougherty, P. D. Kaplan, and J. P. Gollub, *Phys. Rev. Lett.* **58**, 1652 (1987).

<sup>15</sup>S. de Cheveigne, C. Guthmann, and M. M. LeBrun, *J. Cryst. Growth* **73**, 242 (1985), and *J. Phys. (Paris)* **47**, 2095 (1986).

<sup>16</sup>F. Heslot and A. Libchaber, *Phys. Scr.* **T9**, 126 (1985).

<sup>17</sup>J. Bechhoefer and A. Libchaber, *Phys. Rev. B* **35**, 1393 (1987).

<sup>18</sup>A. Chopra, Ph.D. thesis, Rensselaer Polytechnic Institute, 1984 (unpublished); R. Trivedi and K. Somboonsuk, *Mater. Sci. Eng.* **65**, 65 (1984); K. Somboonsuk, J. T. Mason, and R. Trivedi, *Metall. Trans.* **15A**, 967 (1984); R. Trivedi, *Metall. Trans.* **15A**, 977 (1984).

<sup>19</sup>J. D. Hunt, K. A. Jackson, and H. Brown, *Rev. Sci. Instrum.* **37**, 805 (1966).

<sup>20</sup>K. A. Jackson and J. D. Hunt, *Acta Metall.* **13**, 1212 (1965).

<sup>21</sup>AT&T Bell Laboratories Port Scientific Subroutine Library.

<sup>22</sup>C. W. Meyer, G. Ahlers, and D. S. Cannell, *Phys. Rev. Lett.* **59**, 1577 (1987).

<sup>23</sup>Ch. Fattinger, F. Honegger, and W. Lukosz, *Phys. Rev. Lett.* **57**, 2536 (1986).

<sup>24</sup>The use of  $\lambda_{\text{max}}$  from the Mullins-Sekerka theory rather than from the experiment would give  $\rho^*/\lambda_{\text{max}} = 0.13$ .